



Article

# Photosynthetic Picoeukaryotes Diversity in the Underlying Ice Waters of the White Sea, Russia

Tatiana A. Belevich <sup>1,2,\*</sup> , Ludmila V. Ilyash <sup>1</sup>, Irina A. Milyutina <sup>2</sup>, Maria D. Logacheva <sup>2</sup> and Aleksey V. Troitsky <sup>2,\*</sup> 

<sup>1</sup> Biological Faculty, Lomonosov Moscow State University, 119234 Moscow, Russia; ilyash@gmail.ru

<sup>2</sup> Belozersky Institute of Physico-Chemical Biology, Lomonosov Moscow State University, 119992 Moscow, Russia; iramilyutina@yandex.ru (I.A.M.); maria.log@gmail.com (M.D.L.)

\* Correspondence: belevich@mail.bio.msu.ru (T.A.B.); bobr@belozersky.msu.ru (A.V.T.)

Received: 5 February 2020; Accepted: 3 March 2020; Published: 5 March 2020



**Abstract:** The White Sea is a unique basin combining features of temperate and arctic seas. The current state of its biocenoses can serve as a reference point in assessing the expected desalination of the ocean as a result of climate change. A metagenomic study of under-ice ice photosynthetic picoeukaryotes (PPEs) was undertaken by Illumina high-throughput sequencing of the 18S rDNA V4 region from probes collected in March 2013 and 2014. The PPE biomass in samples was 0.03–0.17  $\mu\text{g C}\cdot\text{L}^{-1}$  and their abundance varied from 10 cells·mL<sup>-1</sup> to 140 cells·mL<sup>-1</sup>. There were representatives of 16 algae genera from seven classes and three supergroups, but Chlorophyta, especially Mamiellophyceae, dominated. The most represented genera were *Micromonas* and *Mantoniella*. For the first time, the predominance of *Mantoniella* (in four samples) and Bolidophyceae (in one sample) was observed in under-ice water. It can be assumed that a change in environmental conditions will lead to a considerable change in the structure of arctic PPE communities.

**Keywords:** White Sea; under-ice water; picoeukaryotes; *Micromonas*; *Mantoniella*; high-throughput sequencing; metagenomics; 18S rDNA

## 1. Introduction

The picophytoplankton (cyanobacteria and photosynthetic eukaryotes with cell diameter <3  $\mu\text{m}$ ) make up the smallest component of phytoplankton populations [1–3]. In the Arctic region, photosynthetic picoeukaryotes (PPEs) are major contributors to picophytoplankton and the small phytoplankton (<5  $\mu\text{m}$ ) represent 59%–63% of all marine photosynthetic biomass [4]. The Arctic has been undergoing accelerated warming and freshening since the 1990s due to the melting of multiyear sea ice and increasing river runoff into the Arctic Basin [5,6]. Environmental changes affect the phytoplankton and lead to an increase in PPEs contribution to total primary production and phytoplankton biomass [7–9].

Correct taxonomical identification of PPE requires the use of molecular methods. 18S rRNA gene-based environmental surveys have been increasingly used to investigate the composition of small eukaryotes. Molecular environmental studies conducted in Arctic and subarctic waters reported the presence of diverse microbial communities [10–17]. To better assess the diversity of small photosynthetic eukaryotes, flow cytometry via chlorophyll fluorescence was used to sort cells successfully [16,18–20]. However, the use of flow cytometry does not prevent the detection of heterotrophic eukaryotes that ingest photosynthetic organisms in their food vacuoles and thus could be detected by flow cytometry sorting that targeted chlorophyll fluorescence as well as the detection of photosynthetic algae with cell sizes larger than those of picoforms [20,21]. PPEs in under-ice waters remain understudied, especially for the season preceding the under-ice bloom in spring [10,11,17,22].

The White Sea is a small (area of 90,000 km<sup>2</sup> and volume of 6000 km<sup>3</sup>) subarctic semi enclosed basin with an outlet to the Barents Sea. It has features similar to those of the Arctic shelf seas [23]. Usually from December to May the sea is covered with ice. The White Sea is strongly affected by continental runoff, and its waters are less saline (14–27 psu) than open ocean waters. The species composition and abundance of plankton algae have been studied for almost 80 years in the White Sea [24]. The species richness of nano- and microphytoplankton of the White Sea has been studied by microscopy and is represented by 450 taxa [24]. However, most of the studies examining the taxonomic diversity of the White Sea algae have been limited to the easily recognizable nano- and micro-sized algae, while the PPE composition remained understudied.

Previously, the taxonomic composition of PPEs was studied in summer plankton [25,26] and in the sea ice of the White Sea [27]. PPEs of the White Sea ice were represented by 16 algae genera belonging to eight classes and three supergroups. Chlorophyta, especially Mamiellophyceae, dominated among ice PPEs. The composition of the underlying ice waters' eukaryotic picophytoplankton in the White Sea was estimated for only one sample [28].

Considering the ongoing changes in the Arctic Ocean caused by global warming, and their implications, it is crucial to understand the PPE composition and provide detailed data on the prevalent taxa in subarctic waters. Hence, the objectives of this study were: i) to evaluate under-ice picophytoplankton abundance and biomass and the contribution of PPEs to total picophototroph abundance, ii) to reveal the taxonomic diversity of PPEs during the early spring by way of 18S rDNA sequencing, and iii) to compare the PPEs composition in under-ice water and ice. We targeted the study of the smallest size class of algae by a sample filtration approach, as they are abundant in the Arctic Ocean and difficult to identify by microscopy.

## 2. Materials and Methods

### 2.1. Sampling and Study Area

The samples were collected in Kandalaksha Bay, the White Sea on 19–23 March 2013 and 16–19 March 2014 near the White Sea Biological Station, Lomonosov Moscow State University (66°33' N, 33°06' E), from five different stations (Figure 1) with various degrees of under-ice water salinity and under-ice water current speeds (Table 1). The under-ice water salinity was lower due to the impact of the freshwater runoff at stations 1, 2, and 3 with the maximum freshening level at station 1. Under-ice water at stations 4 and 5 had salinity characteristics of the White Sea surface layer in the winter. The waters at stations 2, 4, and 5 are characterized by higher speeds of under-ice water currents than water areas of stations 1 and 3 [29]. Water samples at stations 1 and 2 were taken twice—in 2013 and 2014. The reference number of each sample consists of the station number, the last two digits of the year when the sample was taken, and the letter “w,” which means water samples (e.g., 1/13w).

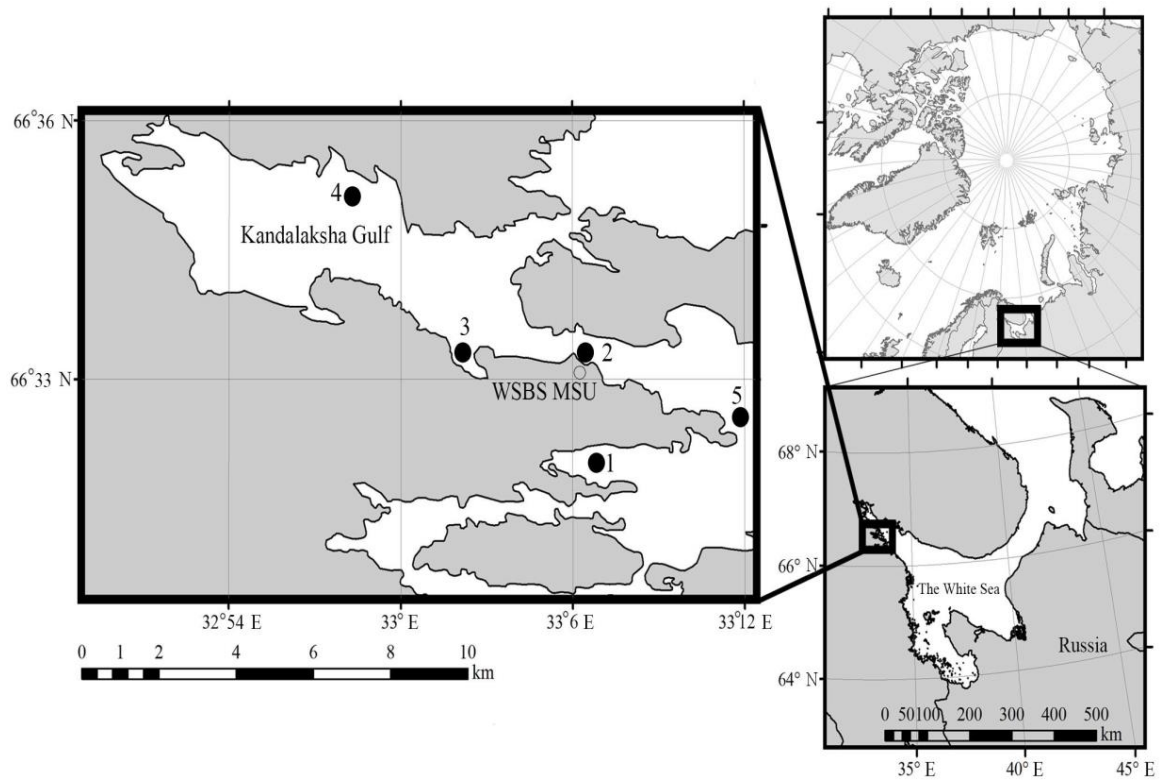


**Figure 1.** Location of the sampling stations in Kandalaksha Bay, White Sea in March 2013 and 2014.

**Table 1.** Characteristics of under-ice waters at the sampling stations of the White Sea: total chlorophyll *a* concentration, the abundance (N) and biomass (B) of photosynthetic picoeukaryotes, and their contribution to total picophytoplankton (including cyanobacteria) abundance (N, %) and biomass (B, %).

Sample	Latitude (N) Longitude (E)	Date	Ice Thickness (cm)	Under Ice Water		Chl- <i>a</i> (µg/L)	N (cells/mL)	B (µg C/L)	N (%)	B (%)
				Salinity (psu)	Temperature (°C)					
1/13w	66°32.01'	19 Mar 2013	71	14.9	−1.0	0.16	140	0.17	11	25
1/14w	33°6.54'	16 Mar 2014	58	15.6	−1.1	0.22	50	0.07	15	35
2/13w	66°33.20'	23 Mar 2013	22	24.5	−0.7	0.05	10	0.06	5	43
2/14w	33°6.28'	17 Mar 2014	49	24.5	−1.2	0.73	20	0.07	33	78
3/14w	66°33.12' 33°2.11'	17 Mar 2014	52	21.9	−0.9	0.32	20	0.03	100	100
4/14w	66°34.87' 32°58.89'	19 Mar 2014	45	26.7	−1.1	0.10	80	0.19	53	86
5/14w	66°32.14' 33°13.17'	15 Mar 2014	26	25.5	−1.2	0.31	10	0.01	5	11

At each station, a titanium manual ice corer (14 cm of diameter) was used to make holes in the ice to collect 5 L of the underlying water. The ice thickness and water temperature were measured. Water temperature was measured directly with a probe Testo 108 (Testo, Lenzkirch, Germany). Within 1 h, water samples were brought to the laboratory, where the salinity was measured with a conductivity probe Cond 3150i (Xylem Analytics Germany Sales GmbH & Co. KG, WTW, Weilheim, Germany). The air temperature recordings from the weather station at the White Sea Biological Station were also used.

## 2.2. Chlorophylla

Subsamples of underlying water (500–1000 mL) were filtered through Whatman GF/F filters and frozen (−80 °C) for subsequent analysis. On returning to the Moscow laboratory, extractions and calculations were made following the procedure [30].

## 2.3. Enumeration of Picophototrophs

Whole (not prefiltered) seawater samples (10 mL) intended for analysis by epifluorescence microscopy were fixed with glutaraldehyde (AppliChem Panreac, Barcelona, Spain) at a final concentration of 1% (*v/v*). Nuclear filters (0.12 µm pore diameter) prestained with Sudan black were used for filtration. Cells with sizes <3 µm were enumerated at × 1000 magnification with a Leica DM2500 (Leica Microsystems GmbH, Wetzlar, Germany) epifluorescence microscope equipped with a 50 W mercury lamp under blue (Filter D; 355–425 nm) and green (Filter N2.1; 515–560 nm) excitation. The bright yellow fluorescence of the phycoerythrin-containing cyanobacteria could be distinguished easily from the deep red fluorescence of the chlorophyll-dominant picoeukaryotes. At least 300 cells at 30–50 microscopic fields were counted for each sample. Cell volumes were calculated as volumes of the relevant geometrical bodies [31] and then converted to their carbon content using the conversion factors of 470 fg C cell<sup>−1</sup> for prokaryotes and 0.433 × (V)<sup>0.863</sup> pg C cell<sup>−1</sup> for PPEs [32].

## 2.4. DNA Isolation of Picoplanktonic Size-fraction

Three to five liters of water samples were filtered through a 2-µm pore size polycarbonate filter and then filtered again through 0.2-µm Sterivex units (Millipore Canada Ltd, Mississauga, ON, Canada). The buffer was added to the Sterivex units (1.8 mL of 50 mM Tris-HCl, 0.75 M sucrose, and 40 mM EDTA; pH 8.3). These units were stored at −80 °C until DNA extraction using the NucleoSpin Plant kit (Macherey-Nagel, Düren, Germany) following the manufacturer's instructions.

## 2.5. DNA Amplification and Sequencing

The ~0.43-kb fragments of the hypervariable V4 region of the 18S rRNA were amplified with the primer pair EuF-V4 (5'-CCAGCASCSCGCGTAATWCC-3') and pico-R2 (5'-AKCCCCYAACTTTTCGTTCTTGAT-3') [27]. For PCR, the Encyclo Plus PCR kit (Evrogen, Moscow, Russia) was used. The volume of the amplification mixture was 30 µL. This was divided into three equal parts (10 µL each), and then PCR was carried out for each sample at three annealing temperatures, 55 °C, 60 °C, and 65 °C [27]. Cycling conditions were as follows: an initial denaturation step for 3 min at 94 °C, followed by 30 cycles (denaturation at 94 °C for 20 s, annealing for 20 s, and extension at 72 °C for 40 s), followed by a final extension at 72 °C for 5 min.

The PCR products obtained at three annealing temperatures were combined and, after extraction by agarose gel electrophoresis, were purified with a Cleanup Mini kit (Evrogen, Moscow, Russia). The resulting amplicons were used to prepare the libraries for the sequencing on the Illumina MiSeq platform (Illumina Inc., San Diego, CA, USA) with a TruSeq Nano DNA Kit (Illumina Inc., San Diego, CA, USA). The maximum read length of the Illumina MiSeq technology is about 500–600 bp, which matches and even exceeds the length of V4 of the SSU rRNA. The hypervariable V4 region of the 18S rRNA revealed an impressive hidden diversity in picoplanktonic communities [3,33].

The effective concentration of the libraries was tested by quantitative PCR with the primers I-qPCR-1.1 (5'-AATGATACGGCGACCACCGAGAT-3') and I-qPCR-2.1 (5'-CAAGCAGAAGACGGCATACGA-3'). The library PhiX Control v3 (Illumina) was used as a control. Then the libraries were diluted to 12 pM and sequenced with a MiSeq Reagent Kit v.2 for 500 cycles. The pair-end read length was  $250 \times 2$  bp.

## 2.6. Bioinformatics and Data Evaluation

The raw sequencing data were processed by Mothur software [34] and other procedures implemented in the SOP protocol [35]. Reads shorter than 150 bp and longer than 550 bp were removed, as well as reads with ambiguous bases (Ns) or >6 repeated bases. Assembled contigs were 430 bp in length, with ~70 bp overlapped paired reads. Identical sequences were removed by the unique.seqs command. The sequences were aligned using MAFFT with FFT-NS-2 strategy, a gap-opening penalty of 1.53, and a gap extension penalty of 0.123. Putative chimeric sequences were identified by UCHIME v 4.2.40 [36] and removed. A distance matrix of the high-quality sequences was constructed, and the sequences were clustered into operational taxonomic units (OTUs) at a 97% similarity level, with average neighbor clustering using cd-hit-est v.3.1.2 [37]. The classification was performed by a local nucleotide BLAST search against the nonredundant version of the SILVA 123 SSU RNA database [38] using blastn (version 2.2.28+) with standard settings [39]. Sequences affiliated with nonprotist phyla or bacteria were eliminated. All singletons were removed. Consensus sequences of the OTUs were generated by the script described earlier [27]. All sequence reads were submitted to the GenBank BioProject (PRJNA368621) under the accession numbers MK571487-MK571523, MN541095, and MN684208. The phylogenetic tree was inferred by maximum likelihood method using RAxML 8.2.10 program [40], with default options according to GTRGAMMA model with 400 bootstrap replications, the number of which was set by bootstrapping criterion implemented in RAxML. The secondary structures of the terminal hairpins of V4 rRNA region were constructed according small subunit RNA secondary structure model [41].

Since the purpose of our research was limited to the photosynthetic picoeukaryotes, from the complete list of taxa revealed in under-ice water samples filtered through a 2- $\mu$ m pore size filter, we chose only those species that have a cell size  $\leq 3$   $\mu$ m. Where OTUs were identified to the genus/order/class level, we only analyzed taxa that, according to the published data [1,42,43], have species corresponding to the pico-size fraction. Since photosynthetic pico-sized cryptophytes were not detected microscopically and photosynthetic pico-sized dinoflagellates are not currently described, these groups were excluded from the analysis. Classes of algae are given according to AlgaeBase [44].

## 2.7. Statistical Procedures

The similarity matrix was calculated after standardization of the abundance of PPEs reads and square-root transformation for reducing the influence of the most dominant taxonomic entries [45]. The PRIMER v6 software (Primer-E Ltd, Plymouth, UK) [46] was used to group samples with similar taxonomic compositions by a group-average linkage cluster analysis and a nonmetric multidimensional scaling (MDS) ordination of a Bray–Curtis similarity matrix [45]. A breakdown of species similarities (SIMPER) was used to determine which taxon combination leads to the resulting groups [47].

## 3. Results

### 3.1. Environmental Conditions

The year 2014 was warmer than 2013 during the sampling period and the preceding month (Figure S1). The air temperature occasionally rose to the water freezing point or above, even in the middle of winter. Kandalaksha Bay was partially ice covered from December, with more complete ice cover in late March in both 2013 and 2014. Ice thickness varied from 22 cm to 71 cm (Table 1). Under-ice water salinity was lowest at station 1 in both years and varied between 14.9 psu and 15.6 psu (Table 1). At

the other stations, the salinity of the under-ice water ranged from 21.9 psu to 26.7 psu. The temperature of the under-ice water varied very little: between  $-0.7$  (2/13w) and  $-1.2$  °C (2/14, 5/14w) with an average of  $-1.0$  °C.

### 3.2. Total Chlorophyll *a* Biomass

Total chlorophyll *a* biomass (Chl *a*) level varied from  $0.05 \mu\text{g}\cdot\text{L}^{-1}$  at sample 2/13w to the highest value of  $0.73 \mu\text{g}\cdot\text{L}^{-1}$  at sample 2/14w (Table 1). The average Chl *a* concentration in under-ice water was  $0.27 \pm 0.21 \mu\text{g}\cdot\text{L}^{-1}$ .

### 3.3. The Abundance of Picophototrophs

The PPEs abundance ranged from  $10 \text{ cells}\cdot\text{mL}^{-1}$  to  $140 \text{ cells}\cdot\text{mL}^{-1}$  with an average of  $50 \text{ cells}\cdot\text{mL}^{-1}$ . The biomass varied between  $0.03$  and  $0.17 \mu\text{g C}\cdot\text{L}^{-1}$  (Table 1). Among photosynthetic pico-sized organisms, cyanobacteria dominated in all samples except 3/14w where we did not reveal photosynthetic prokaryotes. The relative abundance of PPEs varied significantly between 5% and 100% of the total cell counts and carbon biomass of pico-sized photosynthetic organisms.

### 3.4. Taxonomic Composition of Eukaryotes in Samples Filtered through a 2- $\mu\text{m}$ Pore Size Filter

A total of 268,124 amplicons were sequenced from the seven samples, and 122,503 reads remained after quality filtering and preprocessing. The relative abundance of PPEs reads was 11%. The number of OTUs (at the 97% similarity level) that were clustered in individual samples varied between 609 and 3856 (Table 2).

**Table 2.** Summary of recovered reads and the number of operational taxonomic units (OTUs) in under-ice water picoplankton samples.

Sample	Total Number of V4 Tag Sequences	Number of V4 Sequences of Eukaryotes Groups after Quality Filtering	Number of Eukaryotes OTUs (97% Similarity)	Number of PPE Reads	Number of PPE OTUs
1/13w	26,493	7398	609	384	34
2/13w	24,600	19,080	1227	1542	98
1/14w	27,019	12,334	822	1347	72
2/14w	28,525	7645	618	1216	141
3/14w	39,578	17,845	1393	1620	83
4/14w	27,227	7974	738	1101	140
5/14w	94,682	50,227	3856	5947	186
Total	268,124	122,503	9263	13,157	754

Different OTUs are grouped according to their taxonomic affiliations to major phylogenetic groups, such as Chloroplastida, Stramenopiles (Bacillariophyta, Bolidophyceae, Chrysophyceae, Dictyochophyceae, Raphidophyceae, Pelagophyceae, Eustigmatophyceae), Alveolata, Rhizaria, Cryptophyta, Haptophyta, Opisthokonta, and others (Centrohelida, Telonemia, Kathablepharidae, Picozoa, and Eukaryota incertae sedis) (Figure 2). Protists from the taxonomic groups Rhizaria, Opisthokonta, Centrohelida, Telonemia, Kathablepharidae, and Picozoa are nonphotosynthetic forms. Alveolata and Cryptophyta include heterotrophic species. A total of 175 taxa of protists, determined to the genus level, and 148 forms, determined to higher taxonomic ranks, were found in water samples filtered through a 2- $\mu\text{m}$  pore size filter.

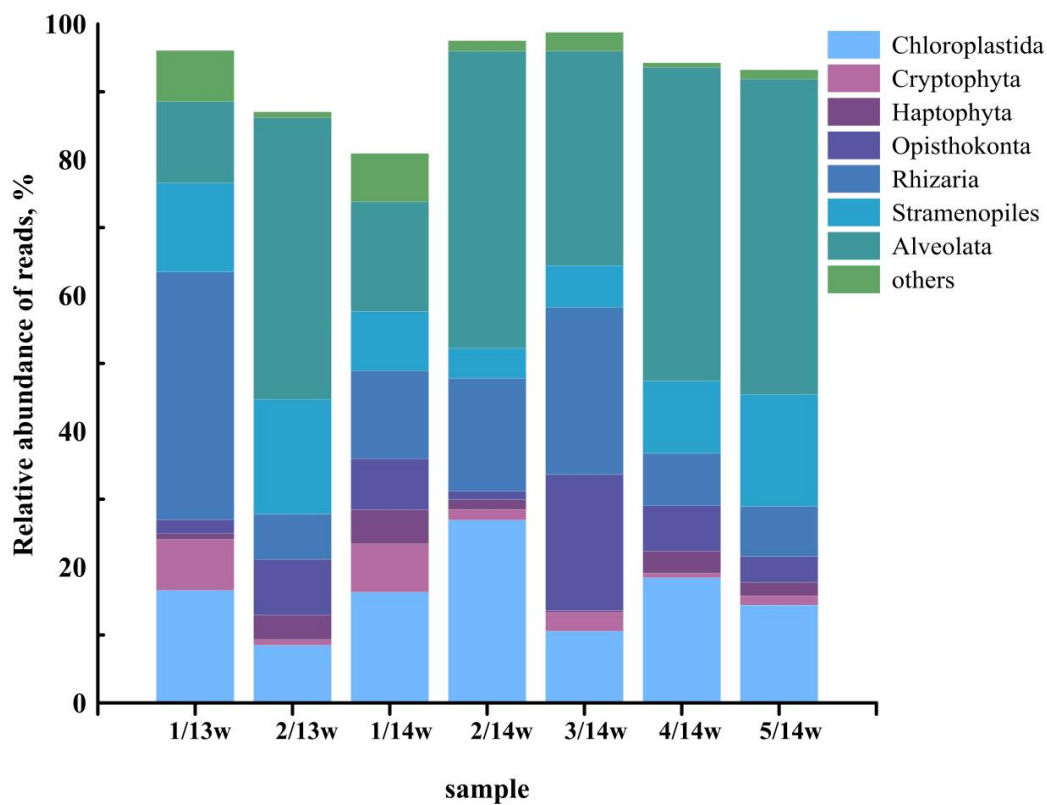


**Figure 2.** The relative abundance (%) of V4 rDNA reads of the major protist groups in picoplankton samples.

### 3.5. OTU Richness and Taxonomic Affiliation of the PPEs Sequences

PPEs belong to three supergroups: Chloroplastida (Chlorophyta), Stramenopiles, and Haptophyta (Table 3). Since different samples yielded different total numbers of sequence reads, they were normalized based on the lowest sample size (sample 1/13w—7398 reads) for comparing OTUs richness. The expected OTUs richness of PPEs was calculated with a 95% probability (Table 3). The minimum expected OTUs richness of PPEs species was observed at the lowest water salinity, in sample 1/13w. The highest expected richness was found at the highest values of salinity, in samples 4/14w and 5/14w.

**Table 3.** Relative abundance (%) of PPE groups based on V4 rDNA reads and the expected OTUs richness of PPEs per sample (95% probability). The standardized number of OTUs for each group is indicated in parentheses.

Taxonomic Group		Reads (%)						
		1/13w	2/13w	1/14w	2/14w	3/14w	4/14w	5/14w
Chloroplastida	Mamiellophyceae	81.2 (59)	27.3 (23)	71.3 (50)	91.8 (89)	82.4 (67)	60.8 (52)	70.2 (56)
	Pyramimonadophyceae	3.9 (6)	0.0	0.0	0.0	0.0	0.0	0.0
	Palmophyllophyceae	0.0	3.6 (3)	0.0	0.0	0.0	1.8 (2)	0.1 (1)
	Trebouxiophyceae	5.0 (6)	1.4 (4)	6.8 (8)	0.2 (1)	4.5 (7)	3.0 (6)	0.2 (1)
Stramenopile	Bolidophyceae	6.8 (21)	58.1 (67)	21.9 (42)	8.1 (12)	13.1 (24)	29.4 (36)	19.6 (39)
	Mediophyceae	0.0	0.0	0.0	0.0	0.0	0.0	0.2 (2)
Haptophyta	Coccolithophyceae	3.1 (9)	9.5 (3)	0.0	0.0	0.0	5.0 (4)	9.7 (2)
Expected OTUs richness of PPEs		36	71	57	105	63	110	103

### 3.6. Chlorophyta

Chlorophyta were represented by four classes: Mamiellophyceae, Pyramimonadophyceae, Palmophyllophyceae, and Trebouxiophyceae (Table 3). Mamiellophyceae were the predominant PPEs



in all samples of under-ice water except sample 2/13w, where Bolidophyceae dominated. Within the Mamiellophyceae, *Micromonas* was the dominant genus in three samples and the *Mantoniella* genus dominated in four samples (Table 4). The negative correlation between the relative abundance of *Micromonas* and *Mantoniella* reads was found ( $R_s = -1$ ;  $p = 0.003$ ). The genera *Ostreococcus*, *Bathycoccus*, *Crustomastix* and OTU similar to the uncultured clone DSGM81 were also detected (Figure 3, Table 5).

**Table 4.** A relative abundance (%) of reads found for different taxonomical groups of Mamiellophyceae based on the V4 region of the 18S rRNA gene sequences.

Taxonomic Group	Reads (%)						
	1/13w	2/13w	1/14w	2/14w	3/14w	4/14w	5/14w
<i>Micromonas polaris</i>	1.6	17.1	1.7	54.9	5.4	66.7	53.1
<i>Micromonas commoda</i> A2	0.0	1.2	0.0	0.0	0.0	0.6	0.5
<i>Micromonas</i> clade F (B3)	0.0	0.7	0.0	0.0	0.0	0.0	0.4
total <i>Micromonas</i>	1.6	19.0	1.7	54.9	5.4	67.3	54.1
<i>Mantoniella squamata</i>	85.2	36.4	11.2	7.9	1.4	4.9	14.6
<i>Mantoniella</i> clade 1	7.7	4.2	42.4	25.8	5.4	8.7	7.1
<i>Mantoniella</i> clade 2	1.3	0.0	13.0	0.6	11.7	0.0	0.0
<i>Mantoniella</i> clade 3	3.5	24.6	30.8	1.4	75.9	8.7	4.5
<i>Mantoniella</i> clade 4	0.0	1.4	0.0	0.0	0.0	0.0	0.0
Total <i>Mantoniella</i>	97.7	66.6	97.4	35.8	94.4	22.3	26.2
<i>Bathycoccus prasinos</i>	0.0	4.7	0.0	0.3	0.0	3.3	2.1
<i>Ostreococcus tauri</i>	0.0	0.0	0.0	0.0	0.0	0.0	0.1
uncultured eukaryotic clone DSGM-81	0.6	9.2	0.9	8.1	0.2	6.7	14.0
<i>Crustomastix</i> sp. MBIC10709	0.0	0.5	0.0	1.0	0.0	0.4	3.6

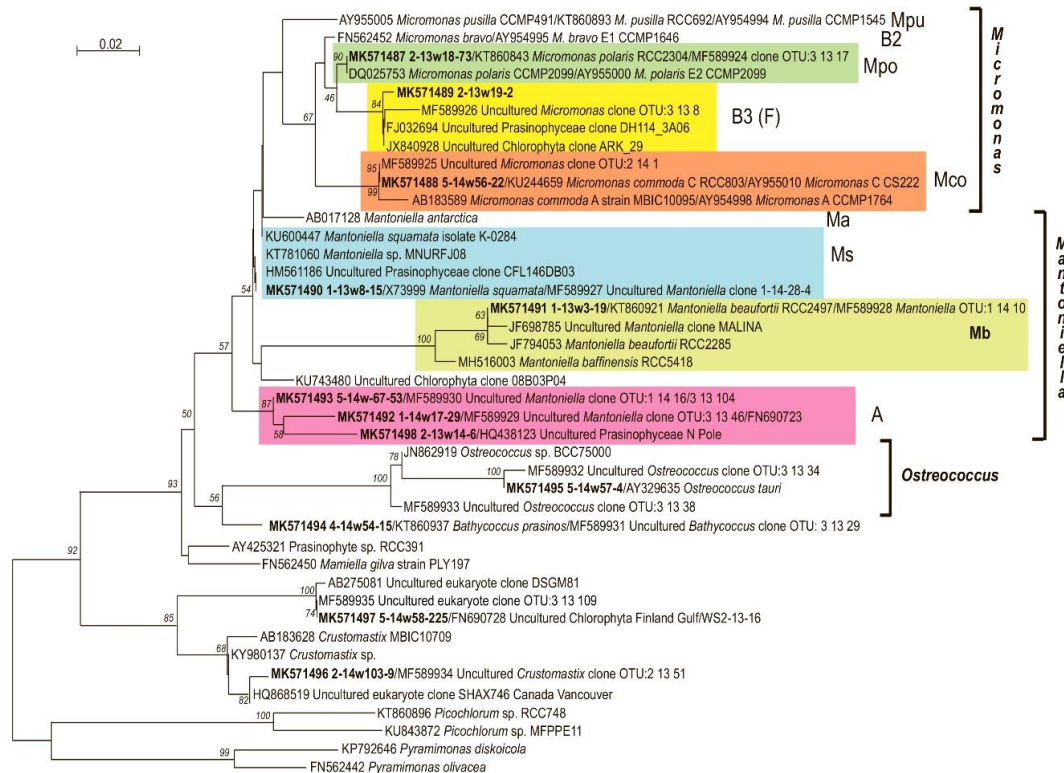


**Figure 3.** Phylogenetic tree of revealed Mamiellophyceae OTUs and Genbank reference sequences constructed from the V4 region of the 18S rRNA gene sequences by the maximum likelihood method. Bootstrap supporting values >0.5 are indicated. The scale is a number of nucleotide substitutions per site. Clades are designated according to Tragin and Vaultot (2019) [43] and Belevich et al. (2018) [27].

**Table 5.** The most abundant PPEs OTUs recovered in the under-ice water of Kandalaksha Bay, the White Sea in March 2013 and 2014 (clustering at 97% similarity threshold). The number of reads of each OTU is indicated in parentheses.

OTU	Closest Match	Identity	Origin
<b>Mamiellophyceae</b>			
2/13w18-73 MK571487	<i>Micromonas pusilla</i> CCMP2099 (clade Ea) AY955000 ( <i>Micromonas polaris</i> )	100%	Baffin Bay, Canada
5/14w56-22 MK571488	<i>Micromonas pusilla</i> strain CS222 (clade C) AY955010 ( <i>Micromonas commoda</i> A2)	100%	South Pacific Ocean
2/13w19-2 MK571489	Uncultured <i>Micromonas</i> clade F MF589926 Uncultured Prasinophyceae clone DH114_3A06 FJ032694 ( <i>Micromonas</i> clade B3)	100%	the White Sea ice South Atlantic Ocean
1/13w8-15 MK571490	<i>Mantoniella squamata</i> X73999 Uncultured Prasinophyceae clone CFL146DB03 HM561186	100%	- the Beaufort Sea
1/13w3-19 MK571491	<i>Mantoniella beaufortii</i> KT860921 Uncultured <i>Mantoniella</i> clade 1 MF589928	100%	the Beaufort Sea the White Sea ice
1/14w17-29 MK571492	Uncultured <i>Mantoniella</i> clade 2 MF589929 Uncultured Chlorophyta clone 5-D5 FN690723	100%	the White Sea ice the Baltic Sea
5/14w67-53 MK571493	Uncultured <i>Mantoniella</i> clade 3 MF589930 Uncultured Chlorophyta clone 5-D5 FN690723	100% 98.4%	the White Sea ice the Baltic Sea
2/13w14-6 MK571498	Uncultured Prasinophyceae clone North_Pole_SI120_29 HQ438123 (uncultured <i>Mantoniella</i> clade 4)	100%	North Pole sea ice
4/14w54-15 MK571494	<i>Bathycoccus prasinos</i> strain RCC801 KT860937	100%	English Channel, Atlantic Ocean
5/14w57-4 MK571495	<i>Ostreococcus tauri</i> Y15814	100%	the Mediterranean Sea
2/14w103-9 MK571496	Uncultured <i>Crustomastix</i> MF589934 Uncultured eukaryote clone SHAX746 HQ868519	100% 99.4%	the White Sea ice Pacific Ocean, Canada
5/14w58-225 MK571497	Uncultured eukaryotic clone DSGM81 AB275081 Uncultured Chlorophyta FN690728	99.2% 100%	methane cold seep sediment (Japan) the Baltic Sea
<b>Pyramimonadophyceae</b>			
1/13w72-12 MK571500	<i>Pyramimonas</i> sp. RCC2009 JF794047	98.1%	the Beaufort Sea
<b>Palmophyllophyceae</b>			
4/14w79-16 MK571499	<i>Prasinoderma coloniale</i> strain RCC854 KT860905 Uncultured eukaryote clone SHAX501 HQ868998	97.0% 98.9%	Pacific Ocean Pacific Ocean, Canada
<b>Trebouxiophyceae</b>			
1/14w39-6 MK571501	<i>Picochlorum</i> sp. RCC748 KT860896	100%	Atlantic Ocean
1/14w40-46 MK571502	<i>Choricystis minor</i> X89012	100%	lake in Germany
<b>Bolidophyceae</b>			
2/13w b284-3 MK571511	<i>Triparma strigata</i> KR998402	100%	Pacific Ocean, Japan
2/13w b270-21 MK571512	Uncultured bolidophyte LC190998	99.0%	Pacific Ocean, Japan
2/13w b264-63 MK571513	Uncultured bolidophyte LC191051	99.0%	Pacific Ocean, Japan
3/14w b337-71 MK571514	Uncultured stramenopile FN690655	99.0%	the Baltic Sea ice
1/14w b286-6 MN684208	Uncultured stramenopile FN690656	100%	the Baltic Sea ice
5/14w b537-30 MK571516	Uncultured eukaryote KT818381	97.8%	the Greenland Sea
4/14w b371-20 MK571518	Uncultured eukaryote KT811782	99.3%	the Greenland Sea
3/14w b346-24 MK571515	Uncultured eukaryote KT814386	98.8%	the Greenland Sea

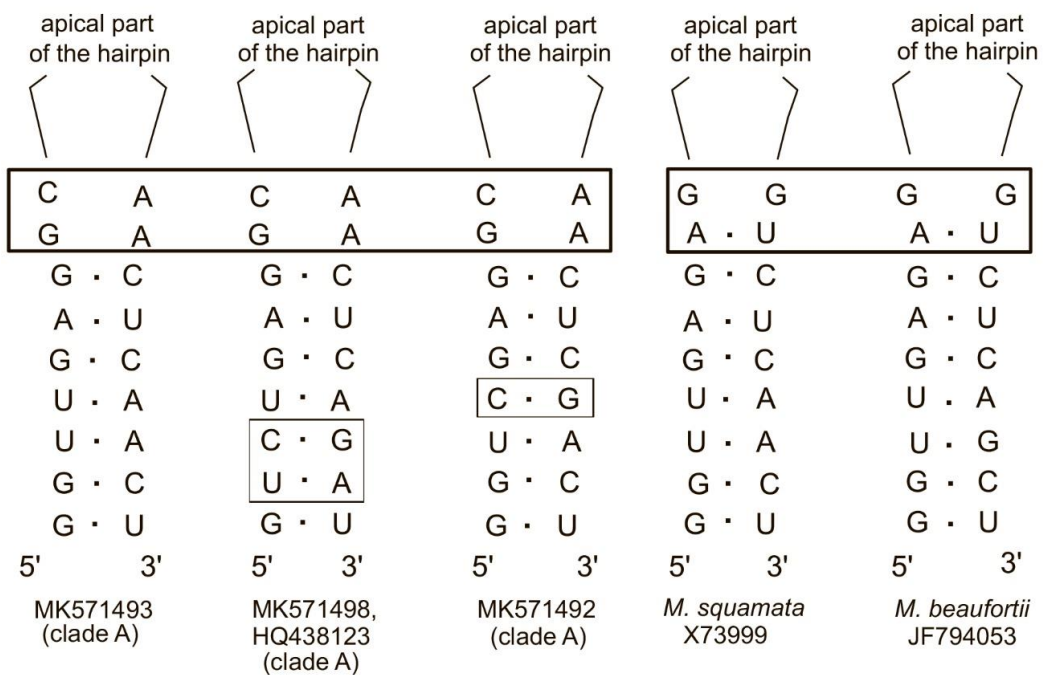
Table 5. Cont.

OTU	Closest Match	Identity	Origin
5/14w b565-83 MK571517	Uncultured eukaryote KT815972	97.8%	the Greenland Sea
2/13w b265-11 MK571519	Uncultured eukaryote KT813573	99.5%	the Greenland Sea
4/14w b360-4 MK571520	Uncultured bolidophyte OTU:b474 MF589906	100%	The White Sea summer water
	Uncultured bolidophyte LC191049	100%	Pacific Ocean
2/13w b282-3 MK571522	Uncultured bolidophyte isolate OTU:b55 MF407369	100%	The White Sea ice
4/14w b397-2 MK571523	Uncultured eukaryote clone 52c_105508 KT814907	99.5%	the Greenland Sea
	Uncultured bolidophyte isolate OTU:b407 MF407373	100%	The White Sea summer water
<b>Mediophyceae</b>			
5/14w120-8 MN541095	<i>Chaetoceros cf. neogracilis</i> strain RCC2318 JN934684	100%	the Beaufort Sea
5/14w103-6 MK571504	<i>Skeletonema marinoi</i> isolate 17 KR091067	100%	Atlantic Ocean
5/14w121-3 MK571505	<i>Minutocellus polymorphus</i> NIES-3970 LC189088	100%	-
	<i>Arcocellulus cornucervis</i> strain RCC2270 JN934677	100%	the Beaufort Sea
<b>Haptophyta</b>			
5/14w130-550 MK571506	<i>Phaeocystis pouchetii</i> isolate AJ01 KR091066	100%	the North Sea
5/14w125-4 MK571507	<i>Chrysochromulina</i> clone MALINA JF698782	98.4%	the Beaufort Sea
2/13w29-6 MK571508	Uncultured eukaryote KP405041	99.2%	the South China Sea
4/14w91-6 MK571509	<i>Chrysochromulina simplex</i> AM491021	99.4%	-
5/14w134-14 MK571510	Uncultured haptophyte Ma135-Pry1-C55 JX680441	100%	the Marmara Sea
	Uncultured haptophyte FN690514	98.7%	the Baltic Sea
	Uncultured haptophyte KC488456	99.2%	the North Atlantic Ocean

The *Micromonas* genus was represented by two species and a recently described clade, corresponding to clade F [27] or clade B3 [43]. *Micromonas polaris* (previously *M. pusilla* clade Ea) was revealed in all samples; its contribution to the total *Micromonas* reads varied between 90% (2/13w) and 100% (1/13w, 1/14w, 2/14w, 3/14w). *Micromonas commoda* clade A2 [43] and *Micromonas* clade F (B3) were revealed much less often—in only three samples (2/13w, 4/14w and 5/14w) and two samples (2/13w and 5/14w), respectively. The contribution of each to the total *Micromonas* reads was low (Table 4).

There were several *Mantoniella* phylotypes from the three clades Ms, Mb, and A in the under-ice water of the White Sea (Figure 3). Three phylotypes were found in all samples: the first was identical to *Mantoniella squamata* (X73999), the second was matched to *Mantoniella beaufortii* (KT860921), and the third from clade A [43] was similar (>98%) to the Uncultured Chlorophyta clone 5-D5 (FN690723) from the Baltic Sea. In general, three phylotypes assigned to clade A were discovered in our samples. Two of them (MK571493 and MK571492) were previously found in the ice of the White Sea and identical to environmental sequences *Mantoniella* MF589930 and *Mantoniella* MF589928, respectively. The third *Mantoniella* phylotype (MK571498), with 100% similarity to the Uncultured Prasinophyceae clone North Pole SI120\_29 (HQ438123) from the marine ice, was revealed in sample 2/13w. Substitutions in basal parts of helixes E23\_1 and H 25 of 18S rRNA are diagnostic for distinguishing the phylotypes *M. squamata* and *M. beaufortii* and three other phylotypes of clade A, MK571493, MK571492, and MK571498 (Figure 4).

### E23-1



### H25

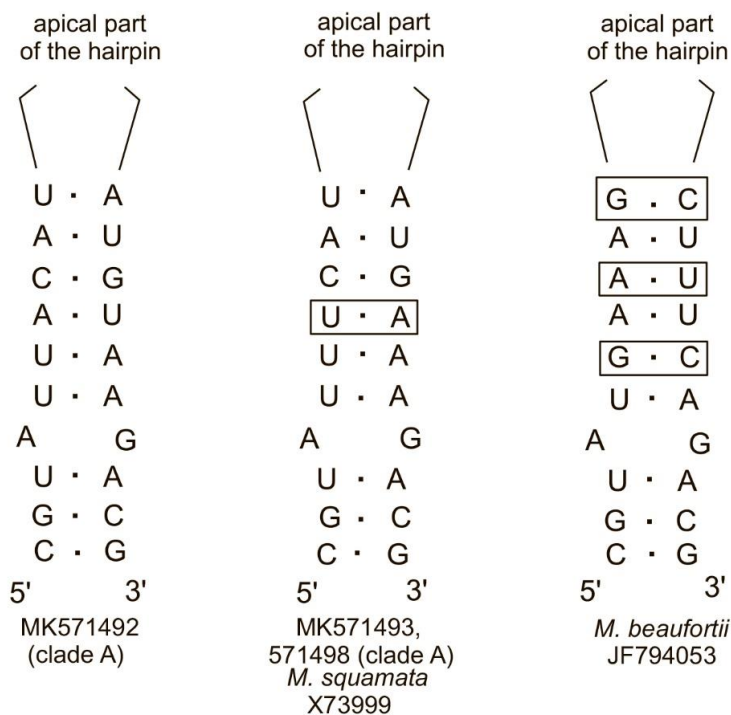


**Figure 4.** Compensatory base changes in the helices of the 18S rRNA secondary structure of *Mantoniella* (helices E23\_1 and H25). The CBCs are shown in rectangles.

*Bathycoccus* OTUs found in samples 2/13w, 2/14w, 4/14w, and 5/14w were identical (100%) to the *Bathycoccus prasinos* strain RCC801 (KT860937). The relative read abundance of *B. prasinos* did not

exceed 5% of Mamiellophyceae reads. The OTU matching *Ostreococcus tauri* (Y15814) was revealed only in sample 5/14w with a low (<1%) relative read abundance. Moreover, in all samples, we revealed OTUs that showed 99.2% similarity to the uncultured eukaryotic clone DSGM-81 (AB275081). The previous molecular phylogenetic analysis revealed that clone DSGM-81 belongs to Mamiellophyceae [27]. *Crustomastix* OTUs were found in four samples and showed 100% similarity to environmental sequences of uncultured *Crustomastix* (MF589934) previously identified in the White Sea ice.

Pyramimonadophyceae sequences were represented by Pyramimonas OTU, which is similar to Pyramimonas sp. (JF794047) from the Beaufort Sea. Among Palmophyllophyceae OTU, Prasinoderma similar to the *Prasinoderma coloniale* strain RCC854 was identified. Trebouxiophyceae from samples 1/13w, 1/14w, and 2/13w were identical to the freshwater algae *Choricystis minor* (X89012). Additionally, in all samples Trebouxiophyceae was represented by OTU identical to *Picochlorum* sp. RCC748 (KT860896) from the Atlantic Ocean.

### 3.7. Stramenopiles

Stramenopiles were represented by two classes: Bolidophyceae and Mediophyceae. All diatoms reads were revealed only in sample 5/14w with the highest sequencing depth. Among Mediophyceae, OTU identical to sequences of two different species, *Minutocellus polymorphus* (LC189088) and *Arcocellulus cornucervis* (JN934677), were revealed. *Skeletonema marinoi* (KR091067) and *Chaetoceros* cf. *neogracilis* (JN934684, KT860998) were also identified.

Bolidophyceae were revealed in all samples (Table 3, Figure 5). They were represented by sequences of *Triparma strigata* (KR998402) with 100% similarity, and OTUs similar to three phylotypes of uncultured bolidophytes earlier revealed in the ice and summer plankton of the White Sea [48], two phylotypes from the plankton of the Pacific Ocean (LC191051, LC190998), two uncultured stramenopiles from the Baltic Sea ice (FN690655, FN690656), and five uncultured eukaryotes from the Greenland Sea (KT818381, KT811782, KT814386, KT815972, and KT813573). Bolidophytes were the predominant PPEs in sample 2/13w.

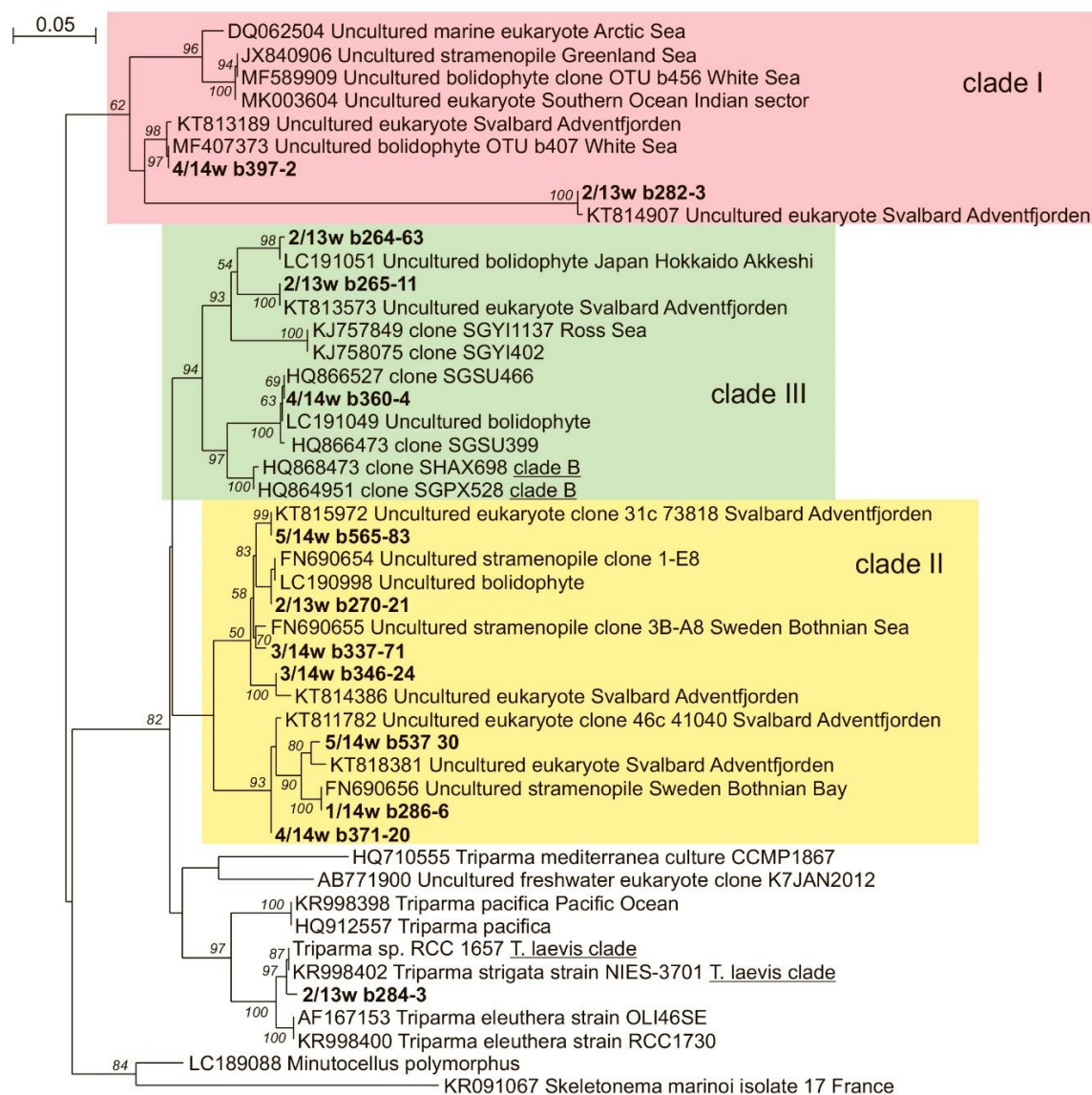


**Figure 5.** The maximum likelihood Bolidophyceae phylogenetic tree constructed from the V4 region of the 18S rDNA. Bootstrap support values >50% are indicated. The scale is the number of nucleotide substitutions per site.

### 3.8. Haptophyta

The contribution of Haptophyta reads varied between 3% and 10% (Table 3). Among the Haptophyta, two genera of class Coccolithophyceae were found—*Phaeocystis* and *Chrysochromulina*. *Phaeocystis* OTUs were similar (>99%) to the *Phaeocystis pouchetii* isolate AJ01 (KR091066) from the North Sea. Sequences closely related to the uncultured *Chrysochromulina* clone MALINA (JF698782) from the Beaufort Sea, occurred at insignificant levels only in the 5/14w sample. *Chrysochromulina simplex* (AM491021) was only found in sample 2/13w. Moreover, two Haptophyta phylotypes were classified at the phylum level with >98% similarity: the uncultured haptophyte (FN690514) from the Baltic Sea and the uncultured haptophyte (KC488456) from the North Atlantic Ocean.

### 3.9. PPEs Community Structure

Contributions of different taxa OTU reads to total numbers of PPE reads resulted in grouping of the stations into two clusters: CI at 64% similarity (1/13w, 1/14w and 3/14w) and CII at 62% similarity

(4/14w, 2/13w, 2/14w and 5/14w) (Figure 6). SIMPER analysis revealed that cluster C1 was characterized by a high contribution of *Mantoniella* reads to the total number of PPEs reads (53%), and cluster C2 was formed by stations with a high contribution of *Micromonas* (22%).

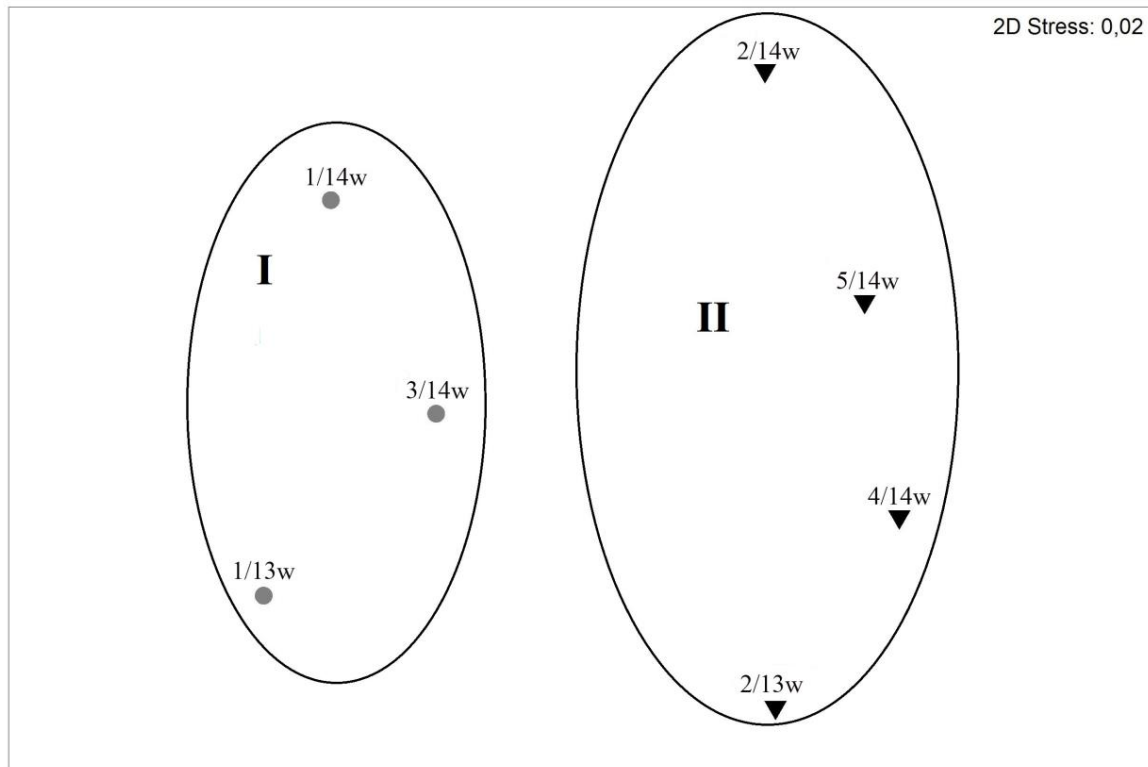


**Figure 6.** Community comparison of PPE assemblages at the different sampling stations using nonmetric multidimensional scaling (MDS) of a data matrix based on Bray-Curtis similarity.

#### 4. Discussion

Our study revealed the most complete genetic diversity of under-ice PPEs in the White Sea, a unique marine environment combining features of temperate and Arctic seas. Such uniqueness of the abiotic environment was reflected in the composition of pico-sized photosynthetic organisms: besides widespread taxa (*Bathycoccus prasinus*, *Ostreococcus tauri*), the Arctic endemic *Micromonas polaris* (previously *M. pusilla* clade E2) and temperate waters *Micromonas commoda* A2 and *Mantoniella* were revealed. Temperate-water taxa survive in the White Sea despite extreme environmental conditions under the ice, i.e., near-freezing temperatures, polar night, and low irradiance, because of the snow and ice cover.

In the under-ice water of Kandalaksha Bay, Chl *a* concentrations in March 2013–2014 were double the values recorded in water samples taken directly underneath the ice of Chupa Inlet of Kandalaksha Bay in February 2002, but half the Chl *a* values in the same inlet in April 2002 [49]. This indicates that our studies of under-ice plankton algae were carried out in the prebloom period. Studies of the biomass plankton algae dynamics from January to April in Kandalaksha Bay also revealed the highest values in April [50]. The values of Chl *a* concentration obtained in the under-ice water of the White Sea are comparable to those in the under-ice water of the Baltic Sea in March (0.5–1.0  $\mu\text{g L}^{-1}$ ) [51].

The abundance of photosynthetic picoeukaryotes in our study was lower than the total number of PPEs observed in ice-covered underlying waters of Kandalaksha Bay (near station 2 in this study) in April 2010 [52]. At the same time, the average PPE abundance was comparable to the numbers of small photosynthetic eukaryotes (<2  $\mu\text{m}$ ) found in the under-ice water of Franklin Bay in December–March, but was approximately one order of magnitude lower than the abundance observed there in April–May [53].

In the under-ice water, PPEs were most abundant in three samples, while cyanobacteria dominated in the biomass in the other four samples. Earlier, the dominance of cyanobacteria was revealed in the summer plankton of the Onega [25] and Kandalaksha [52] bays of the White Sea.

Eukaryotic picoplankton is phylogenetically very diverse and includes lineages not yet described [1,54,55]. High-throughput sequencing of 18S rDNA of pico-sized eukaryotes from under-ice water yielded a detailed view of the plankton PPE community in the ice-covered underlying waters of the subarctic sea. As is commonly found in picoplankton diversity studies based on filtration approaches, sequences from larger protists and metazoans were recovered, probably due to cell breakage and the deformation of flexible walled cells, allowing their DNA and RNA to pass through the 3- $\mu\text{m}$  filters [14,17,27,56]. However, some factors should be noted that can potentially lead to distortions in the estimation of real picoplankton diversity when using filtration. Among them are a probable breakage and deformation of larger cells [14,17,27,56], the presence of extracellular DNA in filtrates [57–59], and inaccurate size-based fraction separation. The metagenomic approach also has its limitations because of possible overestimation of particular OTUs due to high rRNA gene copy numbers or artifacts of the sequencing procedure [60,61], and insufficient 18S rDNA V4 region sequence resolution for detection of all morphospecies, as has been shown for diatoms, for example [62,63]. The exclusion of dinoflagellate sequences from the analysis due to the lack of cultured representatives of this group with cell sizes of less than 3  $\mu\text{m}$  could affect the accuracy of our PPE diversity estimates [1]. Considering the above, 16 algae genera from seven classes and three supergroups are detected among the White Sea under-ice PPEs. Mamiellophyceae dominated in most of the samples. Palmophyllophyceae and Mediophyceae were the minor component of PPEs, Bolidophyceae made a significant contribution and even predominated in one sample.

Most sequences were assigned to Chlorophyta OTUs. Chlorophyta reads were abundant in mid-April during the early phase of the spring bloom in Norwegian waters (Isfjorden, West Spitsbergen) [64]. The dominance of Chlorophyta sequences was repeatedly noted in summer plankton communities of temperate and arctic waters [22,65–67]. On the class level, most Chlorophyta sequences were assigned to Mamiellophyceae OTUs, among which *Micromonas* and *Mantoniella* reads dominated. *Micromonas* was represented by species *Micromonas polaris*, *M. commoda* A2, and a phylotype of a recently described clade F according to Belevich et al. [27], or B3 according to Tragin and Vaultot [43]. *Micromonas polaris* dominated among *Micromonas*. *M. polaris* is widespread and dominant in the under-ice and open Arctic waters [11,17,43,68,69] and regarded as arctic endemic [11,19]. Previously, we detected *M. polaris* (as *Micromonas* E2) in the ice of the White Sea [24]. Its presence in the under-ice water and summer plankton of the subarctic White Sea and the Gulf of Finland of the subarctic Baltic Sea [43] once again indicates that the area of distribution of this species is wider than previously thought [11]. This endemic *M. polaris* does not seem to show intraspecific variability [70].

*Micromonas commoda* was detected earlier in the White Sea ice and summer plankton as *Micromonas* clade C [25,27]. This study is the first to show *M. commoda* in under-ice water. Its relative contribution to total *Micromonas* reads varied from 0% to 6% and was lower than in summer plankton [25]. *M. commoda* has ubiquitous distribution [43,71,72] and constitutes <1%–40% of Mamiellophyceae reads in different regions [43]. Unlike *M. polaris*, which does not show any intraspecific variability, the genetic diversity within *M. commoda* was previously highlighted [43,73,74] and it was suggested that speciation events might be ongoing within this species [72].

This study is the first to discover *Micromonas* clade F (B3) in the under-ice water of the White Sea. Previously, the phylogenetic analysis of Mamiellophyceae revealed the existence of a new clade, *Micromonas* F, in the ice and summer plankton of the White Sea [25,27]. Later, the analysis of the taxonomic diversity and global distribution of *Micromonas* revealed the existence of *Micromonas* clade B3 [43]. This subarctic clade combined amplicons that are 100% similar to OTUs of *Micromonas* clade F from the White Sea ice. *Micromonas* clade B3 made a great contribution to Mamiellophyceae reads from Canada (32%) and amounted to more than 10% of Mamiellophyceae reads at four subarctic stations off Maine and Iceland, as well as at a temperate location off the U.K. coast in the North Sea [43].



The contribution of this taxon to the total Mamiellophyceae reads in under-ice plankton was <1%, which is much lower than in summer plankton [25].

The results of this work represent the first sighting of a broad diversity of *Mantoniella* phylotypes in the under-ice water (Figure 3): *Mantoniella* OTUs match *M. squamata* (clade Ms), *M. beaufortii* (clade Mb), and three other *Mantoniella* lineages from clade A [43] found earlier in the White Sea ice [27]. It has been suggested that clade A is potentially an ice alga [43]. This assumption does not agree with the fact that *Mantoniella* phylotype MK571493 dominated among the Mamiellophyceae reads in two out of seven samples of under-ice water and did not dominate in any of the ice samples [27]. The *Mantoniella* MK571493 and MK571492 are 98.4% similar; however, out of six substitutions making those two phylotypes different from each other, four are compensatory. Likewise, the *Mantoniella* MK571498 sequence is 97.3%–97.8% similar to two other sequences from the same A clade. Substitutions in basal parts of helices E23\_1 and H 25 are differentiated in all known *Mantoniella* phylotypes (Figure 4). Further research may lead to the discovery of new species in the *Mantoniella* A clade.

OTUs of *Ostreococcus* found in the White Sea plankton were identical to the sequence of *O. tauri* Y15814, which was isolated from the Thau lagoon (Mediterranean Sea) with highly variable salinity from 24 to 38 psu [75]. It was suggested that *O. tauri* might represent several species, adapted to different degrees of salinity [43]. The relative abundance of *O. tauri* in under-ice water (<0.1%) was significantly lower than that in summer plankton (31%) [25].

The relative abundance of *Bathycoccus prasinus* reads in under-ice water of the White Sea did not exceed 5%, whereas in summer plankton it reached 33% [25]. *B. prasinus* is a widespread alga with global distribution from tropical to polar waters [43,76]. *Bathycoccus* is now known to be composed of two cryptic species with identical 18S rRNA sequences but differences in the ITS, as well as at the genomic level [76,77]. One of them could be coastal, while another might have adapted to warmer oceanic waters [76–78].

In under-ice water, Palmophyllophyceae and Pyramimonadophyceae were represented only by one taxon each; their respective contributions to total PPEs reads were low. The cell size of *Pyramimonas* sp. (JF794047) is unknown and its assignment to picofoms may be inappropriate. In our samples, several *Pyramimonas* taxa with nanosizes were found (*Pyramimonas mucifera*, *P. olivacea*, *P. tetraarhynchus*, etc.), which is consistent with the high diversity of nanofoms of this genus in arctic and subarctic plankton [19,79].

Trebouxiophyceae were represented by both freshwater *Choricystis minor* and marine *Picochlorum* sp. algae. Its contribution to the total PPEs reads was low (Table 3) and exceed 5% only at station 1 (samples 1/13w and 1/14w), which was most affected by river flows (Table 1). Earlier, the dominance of Trebouxiophyceae reads was revealed in the ice at this station [27].

Diatoms made an insignificant contribution to the PPE community and were found only in sample 5/14 with the maximum sequencing depth. Among all identified diatom taxa, we can confidently assert that only *Minutocellus polymorphus*/*Arcocellulus cornucervis* and *Skeletonema marinoi* match the picofraction. Unfortunately, the resolving power of V4 is insufficient to correctly identify *M. polymorphus* and *A. cornucervis*—their V4 regions are identical [63]. Earlier, *M. polymorphus* was not recorded in the under-ice plankton communities; like *S. marinoi*, it was registered in the sympagic communities of the White Sea [27]. The revealed OTU of *Chaetoceros* cf. *neogracilis* matches two culture representatives of this species deposited in the RCC culture collection (Roscoff, France) numbers RCC2318 and RCC2507. The cell size of both algae is more than 3  $\mu$ . However, small *Chaetoceros* are abundant in spring bloom waters, and the simple morphology could hide a high diversity of species [80,81].

Our study identified a limited variety of Haptophyta in the White Sea under-ice water. We found *Phaeocystis pouchetii* and *Chrysochromulina simplex* that are widespread in the plankton of the subarctic and Arctic seas [19,51,82,83]. The cell sizes of the identified *Chrysochromulina* sp. and two uncultured haptophytes are unknown, but they supposedly can match the size of picofraction. Egge et al. [83] discovered six OTUs assigned to *Chrysochromulina* that were only found in the picoplankton size fraction

rather than the nanoplankton. Since Haptophyta DNA is known to amplify poorly, the molecular methods can underestimate these algae diversity [16,84]. In the Arctic, the number of haptophyte OTUs found in plankton fraction <3 µm varies significantly, between 10–12 in Beaufort Sea and English Channel [16,19] and 59 in the North Pacific [85].

The phylogenetic analysis of Bolidophyceae sequences from the under-ice plankton of the White Sea showed the highest diversity of these algae among the identified PPE classes. Bolidophytes are considered true picosized forms [86]. Bolidophytes were represented by *Triparma strigata* and 12 OTUs of uncultured forms. A large number of bolidophyte sequences are uncultured forms, as noted earlier for the Arctic or subarctic locations, as well as for the Baltic Sea [14,65,79,82,87]. Previously, only two phylotypes of bolidophytes were found in the White Sea [27]. Based on a phylogenetic analysis, the number of White Sea bolidophytes was increased by including sequences from the Genbank that had not been previously classified as Bolidophyceae and had been deposited at the NCBI Genbank as uncultured stramenopile or uncultured eukaryotes [47]. In the under-ice water of the White Sea, four OTUs of bolidophytes have 100% similarity with OTUs found earlier in the ice (1 OTU) and summer plankton (2 OTUs). The phylogenetic analysis recovered that the White Sea bolidophytes refer to three environmental clades (env. clades I, II and III [88] (Figure 4)), in addition to the group corresponding to the genus *Triparma*. Bolidophyte *T. strigata* has a worldwide distribution in plankton and is most abundant in polar waters [89–91]. The complete sequences of the 18S rRNA gene are almost identical (similarity of 99.9%–100%) for such morphologically distinct species as *T. strigata*, *T. laevis f. longispina*, *T. aff. verrucosa*, and flagellate *Triparma* sp. RCC1657; therefore, if only the 18S rRNA gene sequences are considered, all those species are combined in the clade of *T. laevis* [90]. Therefore, the discovery of a phylotype similar to *T. strigata* does not necessarily mean that there is only this species in the under-ice plankton of the White Sea. Bolidophyceae sequences dominated among PPEs reads in sample 2/13. This is the first registration of Bolidophyceae domination in the subarctic plankton.

The dominance of *Micromonas polaris* reads in three out of seven samples corresponds to the fact that our studies were carried out in the prebloom period. *M. polaris* had exceptionally high relative read abundances during pre- and postbloom stages in Isfjorden, West Spitsbergen [64], the Amundsen Gulf, and the Canadian Beaufort Sea [68]. An unexpected result was the high share of different *Mantoniella* taxa in three samples and Bolidophyceae in one sample. Situations where the relative read abundance of *M. polaris* was lower than other taxa were noted earlier in different regions of the Arctic and subarctic: the unexpectedly high proportion of *Bathycoccus* was revealed in July surface samples in the Amundsen Gulf and Canadian Beaufort Sea [68]. It was suggested that this might have been associated with offshore upwelling, or, more speculatively, a viral attack on *Micromonas* triggered by specific oceanographic conditions. *Mantoniella squamata* made a great contribution to the Mamiellophyceae reads off Greenland [43]. The dominance of *Mantoniella* from clade A in PPE reads was identified for the first time. The spatial variability of relative read abundances may be controlled by the combined influence of abiotic and biotic factors.

Earlier, at the same stations as in the present work, we studied the taxonomic composition of PPE and protists in ice samples filtered through a 2-µm pore size filter [27]. Different assemblages colonized the under-ice water and the ice. In samples of under-ice water filtered through a 2-µm pore size filter, Stramenopiles made the most significant contribution to total quality reads (average: 34%), whereas Rhizaria dominated in the ice samples (average: 18%). At the same time, the number of identified protists taxa determined to genus level was comparable: 175 in water and 185 in ice. In the Baltic Sea, the ice community was more diverse than the wintertime water [79]. The contributions of Chloroplastida in ice and water were comparable; the Alveolata contribution was lower in ice than in under-ice water. It is interesting to note that Alveolates were not the dominant group in any of the samples of the White Sea plankton, while the domination of Alveolates in the reads abundance was noted in size-fractionated seawater (0.2–3.0 µm) of the Amundsen Gulf flaw lead system [13].

The similarity of PPE composition in under-ice water and ice was 0.75 (Sørensen index). The variety of phylotypes of certain genera in plankton was lower than in ice. For example, the genus *Ostreococcus*

in plankton was represented only by *O. tauri*, while *O. tauri* and *Ostreococcus* sp. were recorded in ice. Pelagophyceae was found in ice but not in under-ice water. Chlorophyta dominated in both habitats, but the contributions of specific genera and classes varied. For example, the domination of *Mantoniella* in water (three stations) was not observed in the ice, where *Micromonas* always made the most significant contribution. In addition, the domination of Bolidophyceae was observed only in under-ice water (one sample), while the domination of Trebouxiophyceae was only found in ice (one station).

The research undertaken on White Sea under-ice photosynthetic picoeukaryotes' genetic diversity is one stage in studying the dynamics of plankton communities in the subarctic.

**Supplementary Materials:** The following are available online at <http://www.mdpi.com/1424-2818/12/3/93/s1>. Figure S1. Air temperature at the White Sea Biological Station (shaded area corresponds to sampling period).

**Author Contributions:** Conceptualization, T.A.B. and L.V.I.; methodology, M.D.L. and I.A.M.; validation, T.A.B., L.V.I. and A.V.T.; formal analysis, T.A.B., M.D.L. and A.V.T.; investigation, I.A.M. and T.A.B.; resources, T.A.B. and A.V.T.; data curation, I.A.M. and T.A.B.; writing—original draft preparation, T.A.B.; writing—review and editing, A.V.T. and L.V.I.; visualization, A.V.T. and T.A.B.; supervision, A.V.T.; project administration, A.V.T.; funding acquisition, T.A.B. and A.V.T. All authors have read and agreed to the published version of the manuscript.

**Funding:** This study was done in the framework of the Moscow University Project “Noah’s Ark” and of the State Tasks of the Lomonosov Moscow State University (themes no. AAAA-A16-116021660052-0, and AAAA-A17-117120540067-0), with the financial support of the Russian Foundation for Basic Research (project No. 16-05-00502).

**Conflicts of Interest:** The authors declare that they have no conflict of interest.

## References

- Vaulot, D.; Eikrem, W.; Viprey, M.; Moreau, H. The diversity of small eukaryotic phytoplankton (<3 µm) in marine ecosystems. *FEMS Microbiol. Rev.* **2008**, *32*, 795–820. [[CrossRef](#)] [[PubMed](#)]
- Massana, R. Eukaryotic Picoplankton in Surface Oceans. *Annu. Rev. Microbiol.* **2011**, *65*, 91–110. [[CrossRef](#)] [[PubMed](#)]
- Moon-van der Staay, S.Y.; De Wachter, R.; Vaulot, D. Oceanic 18S rDNA sequences from picoplankton reveal unsuspected eukaryotic diversity. *Nature* **2001**, *409*, 607–610. [[CrossRef](#)] [[PubMed](#)]
- Bhavya, P.A.S.; Lee, J.H.; Lee, H.W.; Kang, J.J.; Lee, J.H.; Lee, D.; An, S.H.; Stockwell, D.A.; Whittedge, T.E.; Lee, S.H. First in situ estimations of small phytoplankton carbon and nitrogen uptake rates in the Kara, Laptev, and East Siberian seas. *Biogeosciences* **2018**, *15*, 5503–5517. [[CrossRef](#)]
- Proshutinsky, A.; Krishfield, R.; Timmermans, M.-L.; Toole, J.; Carmack, E.; McLaughlin, F.; Williams, W.J.; Zimmermann, S.; Itoh, M.; Shimada, K. Beaufort Gyre freshwater reservoir: State and variability from observations. *J. Geophys. Res.* **2009**, *114*, 1–25. [[CrossRef](#)]
- Carmack, E.; McLaughlin, F. Towards recognition of physical and geochemical change in Subarctic and Arctic Seas. *Prog. Oceanogr.* **2011**, *90*, 90–104. [[CrossRef](#)]
- Li, W.K.W.; McLaughlin, F.A.; Lovejoy, C.; Carmack, E.C. Smallest algae thrive as the Arctic Ocean freshens. *Science* **2009**, *326*, 539. [[CrossRef](#)]
- Vincent, W.F. Microbial ecosystem responses to rapid climate change in the Arctic. *ISME J.* **2010**, *9*, 1087–1090. [[CrossRef](#)]
- Comeau, A.M.; Li, W.K.W.; Tremblay, J.É.; Carmack, E.C.; Lovejoy, C. Arctic ocean microbial community structure before and after the 2007 record sea ice minimum. *PLoS ONE* **2011**, *6*, e27492. [[CrossRef](#)]
- Lovejoy, C.; Massana, R.; Pedros-Alio, C. Diversity and distribution of marine microbial eukaryotes in the Arctic Ocean and adjacent seas. *Appl. Environ. Microbiol.* **2006**, *72*, 3085–3095. [[CrossRef](#)]
- Lovejoy, C.; Vincent, W.F.; Bonilla, S.; Roy, S.; Martineau, M.-J.; Terrado, R.; Potvin, M.; Massana, R.; Pedros-Alio, C. Distribution, phylogeny, and growth of cold-adapted picoprasinophytes in arctic seas. *J. Phycol.* **2007**, *43*, 78–89. [[CrossRef](#)]
- Hamilton, A.K.; Lovejoy, C.; Galand, P.E.; Ingram, R.G. Water masses and biogeography of picoeukaryote assemblages in a cold hydrographically complex system. *Limnol. Oceanogr.* **2008**, *53*, 922–935. [[CrossRef](#)]
- Terrado, R.; Vincent, W.F.; Lovejoy, C. Mesopelagic protists: Diversity and succession in a coastal Arctic ecosystem. *Aquat. Microb. Ecol.* **2009**, *56*, 25–39. [[CrossRef](#)]

14. Terrado, R.; Medrinal, E.; Dasilva, C.; Thaler, M.; Vincent, W.; Lovejoy, C. Protist community composition during spring in an Arctic flaw lead polynya. *Polar Biol.* **2011**, *34*, 1901–1914. [[CrossRef](#)]
15. Lovejoy, C.; Potvin, M. Microbial eukaryotic distribution in a dynamic Beaufort Sea and the Arctic Ocean. *J. Plankton Res.* **2011**, *33*, 431–444. [[CrossRef](#)]
16. Marie, D.; Shi, X.L.; Rigaut-Jalabert, F.; Vaulot, D. Use of flow cytometric sorting to better assess the diversity of small photosynthetic eukaryotes in the English Channel. *FEMS Microbiol. Ecol.* **2010**, *72*, 165–178. [[CrossRef](#)]
17. Meshram, A.R.; Vader, A.; Kristiansen, S.; Gabrielsen, T.M. Microbial eukaryotes in an Arctic under-ice spring bloom north of Svalbard. *Front. Microbiol.* **2017**, *8*, 1099. [[CrossRef](#)] [[PubMed](#)]
18. Kirkham, A.R.; Jardillier, L.E.; Tiganescu, A.; Pearman, J.; Zubkov, M.V.; Scanlan, D.J. Basin-scale distribution patterns of photosynthetic picoeukaryotes along an Atlantic Meridional Transect. *Environ. Microbiol.* **2011**, *13*, 975–990. [[CrossRef](#)]
19. Balzano, S.; Marie, D.; Gourvil, P.; Vaulot, D. Composition of the summer photosynthetic pico and nanoplankton communities in the Beaufort Sea assessed by T-RFLP and sequences of the 18S rRNA gene from flow cytometry sorted samples. *ISME J.* **2012**, *6*, 1480–1498. [[CrossRef](#)]
20. Kataoka, T.; Yamaguchi, H.; Sato, M.; Watanabe, T.; Taniuchi, Y.; Kuwata, A.; Kawachi, M. Seasonal and geographical distribution of near-surface small photosynthetic eukaryotes in the western North Pacific determined by pyrosequencing of 18S rDNA. *FEMS Microbiol. Ecol.* **2017**, *93*, fiw229. [[CrossRef](#)]
21. Diez, B.; Pedros-Alio, C.; Massana, R. Study of genetic diversity of eukaryotic picoplankton in different oceanic regions by small-subunit rRNA gene cloning and sequencing. *Appl. Environ. Microbiol.* **2001**, *67*, 2932–2941. [[CrossRef](#)] [[PubMed](#)]
22. Metfies, K.; von Appen, W.-J.; Kiliyas, E.; Nicolaus, A.; Nöthig, E.-M. Biogeography and photosynthetic biomass of Arctic marine picoeukaryotes during summer of the record sea ice minimum 2012. *PLoS ONE* **2016**, *11*, e0148512. [[CrossRef](#)] [[PubMed](#)]
23. Berger, V.; Dahle, S.; Galaktionov, K.; Kosobokova, X.; Naumov, A.; Rat'kova, T.; Savinov, V.; Savinova, T. *White Sea: Ecology and Environment*; Derzavets Publisher: St-Petersburg-Tromsø, Russia, 2001.
24. Ilyash, L.V.; Belevich, T.A.; Zhitina, L.S.; Radchenko, I.G.; Ratkova, T.N. Phytoplankton of the White Sea. In *Biogeochemistry of the Atmosphere, Ice and Water of the White Sea: The White Sea Environment Part I*; Lisitzin, A., Gordeev, V., Eds.; Springer: Cham, Switzerland, 2018. [[CrossRef](#)]
25. Belevich, T.A.; Ilyash, L.V.; Milyutina, I.A.; Logacheva, M.D.; Troitsky, A.V. Phototrophic picoeukaryotes of Onega Bay, the White Sea: Abundance and species composition. *Mosc. Univ. Biol. Sci. Bull.* **2017**, *72*, 109–114. [[CrossRef](#)]
26. Milyutina, I.A.; Belevich, T.A.; Ilyash, L.V.; Troitsky, A.V. Insight into picophytoplankton diversity of the subarctic White Sea—The first recording of Pedinophyceae in environmental DNA. *MicrobiologyOpen* **2019**, *8*, e892. [[CrossRef](#)] [[PubMed](#)]
27. Belevich, T.A.; Ilyash, L.V.; Milyutina, I.A.; Logacheva, M.D.; Goryunov, D.V.; Troitsky, A.V. Photosynthetic picoeukaryotes in the land-fast ice of the White Sea, Russia. *Microb. Ecol.* **2018**, *75*, 582–597. [[CrossRef](#)] [[PubMed](#)]
28. Belevich, T.A.; Ilyash, L.V.; Milyutina, I.A.; Logacheva, M.D.; Goryunov, D.V.; Troitsky, A.V. Metagenomic analyses of White Sea picoalgae: First data. *Biochemistry* **2015**, *80*, 1514–1521. [[CrossRef](#)]
29. Pantyulin, A.N. Dynamics, structure, and water masses. In *The White Sea System: Water Column and Interacting Atmosphere, Cryosphere, the River Run-Off, and Biosphere*; Lisitzin, A.P., Ed.; Scientific World: Moscow, Russia, 2012; Volume 2, pp. 309–379. (In Russian)
30. Arar, E.J.; Collins, G.B. Method 445.0. In *In Vitro Determination of Chlorophyll A and Pheophytin A in Marine and Freshwater Algae by Fluorescence*; U.S. Environmental Protection Agency: Washington, DC, USA, 1997.
31. Hillebrand, H.; Dürselen, C.D.; Kirschtel, D.; Pollinger, U.; Zohary, T. Biovolume calculation for pelagic and benthic microalgae. *J. Phycol.* **1999**, *5*, 403–424. [[CrossRef](#)]
32. Verity, P.G.; Robertson, C.Y.; Tronzo, C.R.; Andrews, M.G.; Nelson, J.R.; Sieracki, M.E. Relationship between cell volume and the carbon and nitrogen content of marine photosynthetic nanoplankton. *Limnol. Oceanogr.* **1992**, *37*, 1434–1446. [[CrossRef](#)]
33. López-García, P.; Rodríguez-Valera, F.; Pedrós-Alió, C.; Moreira, D. Unexpected diversity of small eukaryotes in deep-sea Antarctic plankton. *Nature* **2001**, *409*, 603–607. [[CrossRef](#)]

34. Schloss, P.D.; Westcott, S.L.; Ryabin, T.; Hall, J.R.; Hartmann, M.; Hollister, E.B.; Lesniewski, R.A.; Oakley, B.B.; Parks, D.H.; Robinson, C.J.; et al. Introducing mothur: Open-source, platform-independent, community-supported software for describing and comparing microbial communities. *Appl. Environ. Microbiol.* **2009**, *75*, 7537–7541. [[CrossRef](#)]
35. Kozich, J.J.; Westcott, S.L.; Baxter, N.T.; Highlander, S.K.; Schloss, P.D. Development of a dual-index sequencing strategy and curation pipeline for analyzing amplicon sequence data on the MiSeq Illumina sequencing platform. *Appl. Environ. Microbiol.* **2013**, *79*, 5112–5120. [[CrossRef](#)]
36. Edgar, R.C.; Haas, B.J.; Clemente, J.C.; Quince, C.; Knight, R. UCHIME improves sensitivity and speed of chimera detection. *Bioinformatics* **2011**, *27*, 2194–2200. [[CrossRef](#)] [[PubMed](#)]
37. Li, W.; Godzik, A. Cd-hit: A fast program for clustering and comparing large sets of protein or nucleotide sequences. *Bioinformatics* **2006**, *22*, 1658–1659. [[CrossRef](#)] [[PubMed](#)]
38. Quast, C.; Pruesse, E.; Yilmaz, P.; Gerken, J.; Schweer, T.; Yarza, P.; Peplies, J.; Glöckner, F.O. The SILVA ribosomal RNA gene database project: Improved data processing and web-based tools. *Nuc. Acids Res.* **2013**, *41*, D590–D596. [[CrossRef](#)] [[PubMed](#)]
39. Camacho, C.; Coulouris, G.; Avagyan, V.; Ma, N.; Papadopoulos, J.; Bealer, K.; Madden, T. BLAST+: Architecture and applications. *BMC Bioinform.* **2009**, *10*, 421. [[CrossRef](#)] [[PubMed](#)]
40. Stamatakis, A. RAxML version 8: A tool for phylogenetic analysis and post-analysis of large phylogenies. *Bioinformatics* **2014**, *30*, 1312–1313. [[CrossRef](#)] [[PubMed](#)]
41. Wuyts, J.; De Rijk, P.; De Peer, V.Y.; Pison, G.; Rousseeuw, P.; De Wachter, R. Comparative analysis of more than 3000 sequences reveals the existence of two pseudoknots in area V4 of eukaryotic small subunit ribosomal RNA. *Nucleic Acids Res.* **2000**, *28*, 4698–4708. [[CrossRef](#)]
42. Santos, A.L.; Pollina, T.; Gourvil, P.; Corre, E.; Marie, D.; Garrido, J.L.; Rodríguez, F.; Noël, M.-H.; Vaultot, D.; Eikrem, W. Chloropicophyceae, a new class of picophytoplanktonic prasinophytes. *Sci. Rep.* **2017**, *7*, 14019. [[CrossRef](#)]
43. Tragin, M.; Vaultot, D. Novel diversity within marine Mamiellophyceae (Chlorophyta) unveiled by metabarcoding. *Sci. Rep.* **2019**, *9*, 5190. [[CrossRef](#)]
44. Guiry, M.D.; Guiry, G.M. AlgaeBase. World-Wide Electronic Publication, National University of Ireland, Galway. 2017. Available online: <http://www.Algaebase.Org> (accessed on 1 May 2019).
45. Clarke, K.R.; Warwick, R.M. *Change in Marine Communities: An Approach to Statistical Analysis and Interpretation*; Primer-E Ltd.: Plymouth, UK, 2001.
46. Clarke, K.R.; Gorley, R.N. *PRIMER v6: User Manual/Tutorial*; Primer-E Ltd.: Plymouth, UK, 2006.
47. Clarke, K.R. Non-parametric multivariate analyses of changes in community structure. *Aust. J. Ecol.* **1993**, *18*, 117–143. [[CrossRef](#)]
48. Belevich, T.A.; Ilyash, L.V.; Milyutina, I.A.; Logacheva, M.D.; Troitsky, A.V. Metagenomics of Bolidophyceae in plankton and ice of the White Sea. *Biochemistry* **2017**, *82*, 1917–1928. [[CrossRef](#)] [[PubMed](#)]
49. Krell, A.; Ummenhofer, C.; Kattner, G.; Naumov, A.; Evans, D.; Dieckmann, G.S.; Thomas, D.N. The biology and chemistry of land fast ice in the White Sea, Russia – a comparison of winter and spring conditions. *Polar Biol.* **2003**, *26*, 707–719. [[CrossRef](#)]
50. Ilyash, L.V.; Zhitina, L.S.; Kudryavtseva, V.A.; Mel'nikov, I.A. Seasonal dynamics of algae species composition and biomass in the coastal ice of Kandalaksha Bay, the White Sea. *Biol. Bull. Rev.* **2012**, *73*, 459–470. (In Russian)
51. Majaneva, M.; Blomster, J.; Müller, S.; Autio, R.; Majaneva, S.; Hyytiäinen, K.; Nagai, S.; Rintala, J.-M. Sea-ice eukaryotes of the Gulf of Finland, Baltic Sea, and evidence for herbivory on weakly shade-adapted ice algae. *Eur. J. Protistol.* **2017**, *57*, 1–15. [[CrossRef](#)]
52. Belevich, T.A.; Ilyash, L.V. Picophytoplankton abundance in the Velikaya Salma strait, White Sea. *Microbiology* **2012**, *81*, 389–395. [[CrossRef](#)]
53. Terrado, R.; Lovejoy, C.; Massana, R.; Vincent, W.F. Microbial food web responses to light and nutrients beneath the coastal Arctic Ocean sea ice during the winter–spring transition. *J. Mar. Syst.* **2008**, *74*, 964–977. [[CrossRef](#)]
54. Epstein, S.; Lopez-Garcia, P. “Missing” protists: A molecular prospective. *Biodivers. Conserv.* **2008**, *17*, 261–276. [[CrossRef](#)]
55. Massana, R.; Pedros-Alio, C. Unveiling new microbial eukaryotes in the surface ocean. *Curr. Opin. Microbiol.* **2008**, *11*, 213–218. [[CrossRef](#)]

56. Sørensen, N.; Daugbjerg, N.; Gabrielsen, T.M. Molecular diversity and temporal variation of picoeukaryotes in two Arctic fjords, Svalbard. *Polar Biol.* **2012**, *35*, 519–533. [[CrossRef](#)]
57. Nielsen, K.M.; Johnsen, P.J.; Bensasson, D.; Daffonchio, D. Release and persistence of extracellular DNA in the environment. *Environ. Biosaf. Res.* **2007**, *6*, 37–53. [[CrossRef](#)]
58. Charvet, S.; Vincent, W.F.; Comeau, A.; Lovejoy, C. Pyrosequencing analysis of the protist communities in a high Arctic meromictic lake: DNA preservation and change. *Front. Microbiol.* **2012**, *3*, 422. [[CrossRef](#)] [[PubMed](#)]
59. Not, F.; del Campo, J.; Balagué, V.; de Vargas, C.; Massana, R. New Insights into the Diversity of Marine Picoeukaryotes. *PLoS ONE* **2009**, *4*, e7143. [[CrossRef](#)] [[PubMed](#)]
60. Zhu, F.; Massana, R.; Not, F.; Marie, D.; Vaultot, D. Mapping of picoeukaryotes in marine ecosystems with quantitative PCR of the 18S rRNA gene. *FEMS Microb. Ecol.* **2005**, *52*, 79–92. [[CrossRef](#)] [[PubMed](#)]
61. Potvin, M.; Lovejoy, C. PCR-based diversity estimates of artificial and environmental 18S rRNA gene libraries. *J. Eukaryot. Microbiol.* **2009**, *56*, 174–181. [[CrossRef](#)] [[PubMed](#)]
62. Luddington, I.; Kaczmarska, I.; Lovejoy, C. Distance and character-based evaluation of the V4 region of the 18S rRNA gene for the identification of diatoms (Bacillariophyceae). *PLoS ONE* **2012**, *7*, e45664. [[CrossRef](#)] [[PubMed](#)]
63. Balzano, S.; Percopo, I.; Siano, R.; Gourvil, P.; Chanoine, M.; Dominique, M.; Vaultot, D.; Sarno, D. Morphological and genetic diversity of Beaufort Sea diatoms with high contributions from the *Chaetoceros neogracilis* species complex. *J. Phycol.* **2017**, *53*, 161–187. [[CrossRef](#)]
64. Marquardt, M.; Vader, A.; Stübner, E.I.; Reigstad, M.; Gabrielsen, T.M. Strong seasonality of marine microbial eukaryotes in a high-Arctic fjord (Isfjorden, in West Spitsbergen, Norway). *Appl. Environ. Microbiol.* **2016**, *82*, 1868–1880. [[CrossRef](#)]
65. Kiliyas, E.S.; Nöthig, E.M.; Wolf, C.; Metfies, K. Picoeukaryote plankton composition off West Spitsbergen at the Entrance to the Arctic Ocean. *J. Eukaryot. Microbiol.* **2014**, *61*, 569–579. [[CrossRef](#)]
66. Monier, A.; Comte, J.; Babin, M.; Forest, A.; Matsuoaka, A.; Lovejoy, C. Oceanographic structure drives the assembly processes of microbial eukaryotic communities. *ISME J.* **2015**, *9*, 990–1002. [[CrossRef](#)]
67. Zhang, F.; He, J.; Lin, L.; Jin, H. Dominance of picophytoplankton in the newly open surface water of the central Arctic Ocean. *Polar Biol.* **2015**, *38*, 1081–1089. [[CrossRef](#)]
68. Joli, N.; Monier, A.; Logares, R.; Lovejoy, C. Seasonal patterns in Arctic prasinophytes and inferred ecology of *Bathycoccus* unveiled in an Arctic winter metagenome. *ISME J.* **2017**, *11*, 1372–1385. [[CrossRef](#)]
69. Kiliyas, E.; Wolf, C.; Nöthig, E.M.; Peeken, I.; Metfies, K. Protist distribution in the western Fram Strait in summer 2010 based on 454-pyrosequencing of 18S rDNA. *J. Phycol.* **2013**, *49*, 996–1010. [[CrossRef](#)] [[PubMed](#)]
70. Balzano, S.; Gourvil, P.; Siano, R.; Chanoine, M.; Marie, D.; Lessard, S.; Sarno, D.; Vaultot, D. Diversity of cultured photosynthetic flagellates in the northeast Pacific and Arctic Oceans in summer. *Biogeosciences* **2012**, *9*, 4553–4571. [[CrossRef](#)]
71. Foulon, E.; Not, F.; Jalabert, F.; Cariou, T.; Massana, R.; Simon, N. Ecological niche partitioning in the picoplanktonic green alga *Micromonas pusilla*: Evidence from environmental surveys using phylogenetic probes. *Environ. Microbiol.* **2008**, *10*, 2433–2443. [[CrossRef](#)]
72. Simon, N.; Foulon, E.; Grulois, D.; Six, C.; Desdevises, Y.; Latimier, M.; Le Gall, F.; Tragin, M.; Houdan, A.; Derelle, E.; et al. Revision of the genus *Micromonas* Manton et Parke (Chlorophyta, Mamiellophyceae), of the type species *M. pusilla* (Butcher) Manton & Parke and of the species *M. commoda* van Baren, Bachy and Worden and description of two new species based on the genetic and phenotypic characterization of cultured isolates. *Protist* **2017**, *168*, 612–635. [[CrossRef](#)] [[PubMed](#)]
73. Slapeta, J.; López-García, P.; Moreira, D. Global dispersal and ancient cryptic species in the smallest marine eukaryotes. *Mol. Biol. Evol.* **2006**, *23*, 23–29. [[CrossRef](#)]
74. Worden, A.Z.; Lee, J.-H.; Mock, T.; Rouzé, P.; Simmons, M.P.; Aerts, A.L.; Allen, A.E.; Cuvelier, M.L.; Derelle, E.; Everett, M.V.; et al. Green evolution and dynamic adaptations revealed by genomes of the marine picoeukaryotes *Micromonas*. *Science* **2009**, *324*, 268–272. [[CrossRef](#)]
75. Courties, C.; Perasso, R.; Chrétiennot-Dinet, M.-J.; Gouy, M.; Guillou, L.; Troussellier, M. Phylogenetic analysis and genome size of *Ostreococcus tauri* (Chlorophyta, Prasinophyceae). *J. Phycol.* **1998**, *34*, 844–849. [[CrossRef](#)]

76. Vannier, T.; Leconte, J.; Seeleuthner, Y.; Mondy, S.; Pelletier, E.; Aury, J.-M.; de Vargas, C.; Sieracki, M.; Iudicone, D.; Vaulot, D.; et al. Survey of the green picoalga *Bathycoccus* genomes in the global ocean. *Sci. Rep.* **2016**, *6*, 37900. [[CrossRef](#)]
77. Vaulot, D.; Lepère, C.; Toulza, E.; De la Iglesia, R.; Poulain, J.; Gaboyer, F.; Moreau, H.; Vandepoele, K.; Ulloa, O.; Gavory, F.; et al. Metagenomes of the picoalga *Bathycoccus* from the Chile Coastal Upwelling. *PLoS ONE* **2012**, *7*, e39648. [[CrossRef](#)]
78. Limardo, A.J.; Sudek, S.; Choi, C.J.; Poirier, C.; Rii, Y.M.; Blum, M.; Roth, R.; Goodenough, U.; Church, M.J.; Worden, A.Z. Quantitative biogeography of picoprasinophytes establishes ecotype distributions and significant contributions to marine phytoplankton. *Environ. Microbiol.* **2017**, *19*, 3219–3234. [[CrossRef](#)] [[PubMed](#)]
79. Majaneva, M.; Rintala, J.M.; Piisila, M.; Fewer, D.P.; Blomster, J. Comparison of wintertime eukaryotic community from sea ice and open water in the Baltic Sea, based on sequencing of the 18S rRNA gene. *Polar Biol.* **2012**, *35*, 875–889. [[CrossRef](#)]
80. Booth, B.C.; Larouche, P.; Belanger, S.; Klein, B.; Amiel, D.; Mei, Z.P. Dynamics of *Chaetoceros socialis* blooms in the North Water. *Deep Sea Res. II Top. Stud. Oceanogr.* **2002**, *49*, 5003–5025. [[CrossRef](#)]
81. Degerlund, M.; Eilertsen, H.C. Main species characteristics of phytoplankton spring blooms in NE Atlantic and Arctic waters (68–80° N). *Estuar. Coast. Shelf Sci.* **2010**, *33*, 242–269. [[CrossRef](#)]
82. Dasilva, C.R.; Li, W.K.W.; Lovejoy, C. Phylogenetic diversity of eukaryotic marine microbial plankton on the Scotian Shelf, Northwestern Atlantic Ocean. *J. Plankton Res.* **2013**, *36*, 344–363. [[CrossRef](#)]
83. Egge, E.S.; Johannessen, T.V.; Andersen, T.; Eikrem, W.; Bittner, L.; Larsen, A.; Sandaa, R.A.; Edvardsen, B. Seasonal diversity and dynamics of haptophytes in the Skagerrak, Norway, explored by high-throughput sequencing. *Mol. Ecol.* **2015**, *24*, 3026–3042. [[CrossRef](#)]
84. Liu, H.; Probert, I.; Uitz, J.; Claustre, H.; Aris-Brosou, S.; Frada, M.; Not, F.; Vargas, C. Extreme diversity in noncalcifying haptophytes explains a major pigment paradox in open oceans. *Proc. Natl. Acad. Sci. USA* **2009**, *106*, 12803–12808. [[CrossRef](#)]
85. Orsi, W.; Song, Y.C.; Hallam, S.; Edgcomb, V. Effect of oxygen minimum zone formation on communities of marine protist. *ISME J.* **2012**, *6*, 1586–1601. [[CrossRef](#)]
86. Ichinomiya, M.; Yoshikawa, S.; Kamiya, M.; Ohki, K.; Takaichi, S.; Kuwata, A. Isolation and characterization of Parmales (Heterokonta/Heterokontophyta/Stramenopiles) from the Oyashio region, Western North Pacific. *J. Phycol.* **2011**, *47*, 144–151. [[CrossRef](#)]
87. Ichinomiya, M.; dos Santos, A.; Gourvil, P.; Yoshikawa, S.; Kamiya, M.; Ohki, K.; Audic, S.; de Vargas, C.; Noël, M.-H.; Vaulot, D.; et al. Diversity and oceanic distribution of the Parmales (Bolidophyceae), a picoplanktonic group closely related to diatoms. *ISME J.* **2016**, *10*, 2419–2434. [[CrossRef](#)]
88. Kuwata, A.; Yamada, K.; Ichinomiya, M.; Yoshikawa, S.; Tragin, M.; Vaulot, D.; dos Santos, A. Bolidophyceae, a Sister Picoplanktonic Group of Diatoms—A Review. *Front. Mar. Sci.* **2018**, *5*, 370. [[CrossRef](#)]
89. Komuro, C.; Narita, H.; Imai, K.; Nojiri, Y.; Jordan, R.W. Microplankton assemblages at Station KNOT in the subarctic western Pacific, 1999–2000. *Deep Sea Res. II Top. Stud. Oceanogr.* **2005**, *52*, 2206–2217. [[CrossRef](#)]
90. Ichinomiya, M.; Nakamachi, M.; Shimizu, Y.; Kuwata, A. Growth characteristics and vertical distribution of *Triparma laevis* (Parmales) during summer in the Oyashio region, western North Pacific. *Aquat. Microb. Ecol.* **2013**, *68*, 107–116. [[CrossRef](#)]
91. Pivosz, K.; Wiktor, J.M.; Niemi, A.; Tatarek, A.; Michel, C. Mesoscale distribution and functional diversity of picoeukaryotes in the first-year sea ice of the Canadian Arctic. *ISME J.* **2013**, *7*, 1461–1471. [[CrossRef](#)]

